AWARD NUMBER: W81XWH-17-1-0146

TITLE: The Role of Mesothelial Omentin in Ovarian Cancer Progression

PRINCIPAL INVESTIGATOR: Kay-Pong Yip

CONTRACTING ORGANIZATION: University of South Florida

REPORT DATE: May 2020

TYPE OF REPORT: Annual

PREPARED FOR: U.S. Army Medical Research and Materiel Command
Fort Detrick, Maryland 21702-5012

DISTRIBUTION STATEMENT: Approved for Public Release;
Distribution Unlimited

REPORT DOCUMENTATION PAGE

Form Approved
OMB No. 0704-0188

1. REPORT DATE	2. REPORT TYPE	3. DATES COVERED
May 2020	Annual	5/1/2019-4/30/2020

4. TITLE AND SUBTITLE

The role of mesothelial omentin in ovarian cancer progression

5a. CONTRACT NUMBER

5b. GRANT NUMBER
W81XWH-17-1-0146

5c. PROGRAM ELEMENT NUMBER

6. AUTHOR(S)
Kay-Pong Yip

E-Mail:dyip@health.usf.edu

5d. PROJECT NUMBER

5e. TASK NUMBER

5f. WORK UNIT NUMBER

7. PERFORMING ORGANIZATION NAME(S) AND ADDRESS(ES)

University of South Florida
4202 E. Fowler Ave.
Tampa FL 33620-9951

8. PERFORMING ORGANIZATION REPORT NUMBER

9. SPONSORING / MONITORING AGENCY NAME(S) AND ADDRESS(ES)

U.S. Army Medical Research and Materiel Command
Fort Detrick, Maryland 21702-5012

10. SPONSOR/MONITOR'S ACRONYM(S)

11. SPONSOR/MONITOR'S REPORT NUMBER(S)

12. DISTRIBUTION / AVAILABILITY STATEMENT

Approved for Public Release; Distribution Unlimited

13. SUPPLEMENTARY NOTES

14. ABSTRACT

We hypothesize that omentin (ITLN1) suppresses ovarian cancer progression by sequestering lactotransferrin (LTF) from its receptor (LRP1) on the ovarian cancer cells and adipocytes, and that lactotransferrin promotes ovarian cancer cells motility and growth. The most significant finding in this research period are (1) exogenous omentin suppresses ovarian cancer cells' motility and invasive potential, (2) matrix etalloproteinase-1 (MMP1) mediated the effects of omentin on suppressing ovarian cancer cells' motility and invasive potential, (3) ITLN1 abrogates LTF's effects on ovarian cancer cells' motility and invasive potential (4) omentin suppressed ovarian cancer growth by enhancing insulin-dependent glucose in adipocytes via facilitative glucose transporter (GLUT4/SLC2A4), and (5) exogenous omentin suppressed ovarian cancer progression in vivo.

15. SUBJECT TERMS
Ovarian cancer, omentin, lactoferrin, mesothelium, tumor microenvironment

16. SECURITY CLASSIFICATION OF:			17. LIMITATION OF ABSTRACT	18. NUMBER OF PAGES	19a. NAME OF RESPONSIBLE PERSON
a. REPORT	b. ABSTRACT	c. THIS PAGE			USAMRMC
Unclassified	Unclassified	Unclassified	Unclassified	24	19b. TELEPHONE NUMBER *(include area code)*

Standard Form 298 (Rev. 8-98)
Prescribed by ANSI Std. Z39.18

Table of Contents

1. INTRODUCTION

Advanced epithelial ovarian cancer occurs most frequently in postmenopausal women and metastasizes preferentially to the soft omentum. The omentum is covered by a layer of mesothelial cells. Disseminated ovarian cancer cells must adhere to and invade through the mesothelial cell layer before developing as metastasized tumor nodules in the omentum. However, the exact role of mesothelial cells in ovarian cancer cell adhesion and growth is unclear. Alteration in gene expression in mesothelial cells by ovarian cancer cells may facilitate the adhesion and progression of ovarian cancer cells. Using RNAseq analysis on mesothelial cells co-cultured with ovarian cancer cells, we identified a differential gene signature for ovarian cancer associated mesothelial cells. One of the most significantly down regulated genes in mesothelial cells co-cultured with ovarian cancer cells is interlectin-1 (ITLN1), also known as omentin. Omentin is a 38 kDa secreted protein and can bind and sequester lactotransferrin from its receptors. Lactotransferrin (LTF) is known to trigger FAK, Erk1/2 and Akt dependent signaling processes through its receptor, low density lipoprotein receptor-related protein-1 (LPR1), which might stimulate ovarian cancer cell proliferation and invasiveness. Western blot analyses confirmed omentin was down-regulated in mesothelial cells obtained from patients with ovarian cancers compared to body mass index (BMI) matched healthy individuals. Circulating omentin levels is significantly lower in patients with high-grade serous ovarian cancer (HGSOC) compared with those in BMI matched healthy individuals. Survival correlation studies demonstrated that high levels of pre-operative serum omentin (>350 ng/ml) in patients with high-grade serous ovarian cancer were associated with longer survival times. Our preliminary data showed that omentin significantly lowered the number of ovarian cancer cells adhering to the mesothelial cell monolayer. Omentin alone did not inhibit ovarian cancer growth. However, conditioned media collected from adipocytes treated omentin inhibited the growth of ovarian cancer cells, which suggested that omentin inhibited ovarian cancer growth only in the presence of adipocytes.

Based on our preliminary studies, we hypothesize that cancer or stromal cells in the omental tumor microenvironment produce tumor specific mediators down-regulate omentin expression in the mesothelial cells covering the omental adipose tissue, which subsequently facilitates ovarian tumor progression. Since secreted omentin binds lactotransferrin, it can sequester lactotransferrin from its receptor LRP1 on ovarian cancer cells and adipocytes. Unopposed lactotransferrin due to down-regulation of omentin results in the activation of LPR1 mediated downstream signaling events in the ovarian cancer cells, which confers a more aggressive ovarian cancer cell phenotype, and leads to poor clinical outcomes. Strategies that aim to increase omentin levels in patients should therefore suppress ovarian cancer progression and improve survival.

2. KEYWORDS

Ovarian cancer, omentin, lactotransferrin, mesothelium, tumor microenvironment

3. ACCOMPLISHMENTS

a. What were the major goals of the project?

Specific Aim 1

Major Task 1: Measure changes in cytosolic Ca^{2+} and cell traction force in cancer cells induced by lactotransferrin (Months 1-9).

Major Task 2: Evaluate the effects of lactotransferrin and omentin on MMP1 expression in ovarian cancer cells. (Months 10-18).

Major Task 3: Evaluate the role of store-operated Ca^{2+} entry (SOCE) in ovarian cancer cell motility and invasion potential. (Months 19-25).

Major Task 4: Evaluate the effects of lactotransferrin and omentin on the invasion of ovarian cancer cells into mesothelial cells (Months 26-34).

Specific Aim 2

Major Task 1: Evaluate the effects of omentin on insulin dependent glucose uptake in adipocytes, and test whether omentin suppress ovarian cancer growth by glucose deprivation. (Months 1-6).

Major Task 2: Evaluate whether glucose deprivation plays a role in suppressing tumor growth in the omental tumor microenvironment using Induced Metabolic Bioluminescence Imaging (Months 7-14).

Major Task 3: Evaluate the effects of lactotransferrin and omentin on GLUT4 expression of (Months 15-21).

Specific Aim 3.

Major Task 1: Boost circulating omentin levels in C57BL/6 mice using adeno-associated virus (AAV). (Months 1-24).

Major Task 2: To evaluate the therapeutic potential of recombinant omentin. (Months 25-34).

b. What was accomplished under these goals?

Specific Aim 1 Major Task 1 : We demonstrated that lactotransferrin (LTF) can trigger Ca^{2+} dependent signal cascade in ovarian cancer cells and increase of cell traction force, we monitored the effects of lactotransferrin in cytosolic Ca^{2+} mobilization and the amplitude of cell traction force in ovarian cancer cell lines (A224, OVA433, and SKOV3) using confocal fluorescence microscopy and traction force microscopy. The results demonstrated that lactoferrin can trigger cytosolic Ca^{2+} mobilizations and increase of cell traction in all three cell lines tested. Data extracted from ovarian cancer cell line A224 are shown in Figures 1 and 2.

Specific Aim 1 Major Task 2: To determine the molecular mechanism by which ITLN1 suppresses ovarian cancer cells' motility and invasive potential, we performed transcriptome profiling on ovarian cancer A224 cells treated with exogenous ITLN1 (Figure 3A). To uncover the biological functions of the ITLN1-induced gene expression profile that are associated with cell motility and invasive potential, we used Ingenuity Pathway Analysis to analyze the list of differentially expressed genes in A224 cells treated with exogenous ITLN1. One predicted activated biological function associated with cell motility and invasive potential was identified (Activation Z-score=-1.585; p=4.92E-05). From the list of genes associated with cell motility and invasive potential, we selected MMP1 (Interstitial collagenase), one of the MMP family members that has long been associated with invasion and metastasis for further studies. QRT-PCR and Western blot analyses on SKOV3 and A224 cells treated with ITLN1 or PBS confirmed that MMP1 mRNA and protein were downregulated in cells treated with ITLN1 compared with those threated with PBS. (Figures 3B and 3C). These data suggest that MMP1 plays a role in mediating ITLN1's effect on ovarian cancer cell motility and invasion potential.

Next, we evaluated whether LTF can upregulate MMP1 expression in ovarian cancer cells. When SKOV3 and A224 cells were treated with LTF (100 µg/mL) in serum-free media, we found a significant increase in MMP1 mRNA and protein expression in both cell lines (Figures 4A and 4B). When these cells were transfected with either MMP1-specific siRNAs or the control siRNA and then treated with LTF, the stimulating effects of LTF on cell motility were abrogated (Figure 4C), suggesting that the effects of LTF on ovarian cancer motility and invasion potential are mediated through MMP1. Subsequently, both SKOV3 and A224 cells were treated with LTF in the presence of different concentrations of ITLN1 (100 and 1000 ng/mL). The results showed that ITLN1 abrogated the effect of LTF on MMP1 expression in a dose-dependent manner (Figure 4A), suggesting that ITLN1 attenuates the promoting effect of LTF on MMP1 expression in ovarian cancer cells, and thus suppresses ovarian cancer motility and invasion potential.

Specific Aim 1 Major Task 3. We have demonstrated store-operated calcium entry (SOCE) in multiple ovarian cancer cell lines including A224, SKOV3, OVAC432 and OVCA433. We did not pursue this Task 3 further because other groups have addressed similar questions have published their observations during this grant period. Their observations demonstrated that SOCE can modulate ovarian cancer cell motility and invasion. (Hunag et al. J. Biomed. Sci. 2020).

Specific Aim 1 Major Task 4. The focus of this task was shifted to delineate the cellular mechanisms of how ITLN1 counters the cellular signals triggered by LFT in ovarian cancer cell motility and invasion, instead of simply to monitor the invasion of ovarian cancer cells into mesothelial cells.

To determine the signaling network by which ITLN1 downregulates MMP1, we sought to identify molecules or receptors that had been shown to interact with ITLN1. A literature search did not identify any functional receptors that bind to ITLN1; however, the membrane-bound form of ITLN1 has been shown to interact with lactotransferrin (LTF). In addition, it has been shown that LTF's binding to one of its receptors, LRP1 (low-intensity lipoprotein-receptor-related protein 1), transcriptionally upregulates MMP1. We therefore hypothesized that ITLN1 binds to LTF, which prevents LTF from binding to its receptor LRP1 on ovarian cancer cells and, subsequently leads to the downregulation of MMP1. To test this hypothesis, we first needed to confirm that ITLN1 binds to LTF and to determine whether ITLN1 blocks the interaction between LTF and LRP1. Accordingly, we performed an i*n vitro* pull-down assay on purified LTF and recombinant ITLN1 in serum-free media to confirm that ITLN1 interacts with LTF. A Western blot analysis, in which we used anti-ITLN1 antibody on proteins pulled down by an anti-LTF antibody showed a 34 kDa ITLN1 band (Figure 5A), suggesting that ITLN1 binds to LTF. To determine whether ITLN1 can interfere with the binding of LTF to LRP1 on ovarian cancer cells, we performed a Duolink proximity ligation assay using both anti-LTF and anti-LRP1 antibodies. The results showed that there was a significant decrease in fluorescent signals in cells that were treated with ITLN1 compared with those that were not (Figure 5B). Taken together, these data suggest that ITLN1 interacts with LTF and prevents LTF from binding to its receptor LRP1 on ovarian cancer cells.

To determine whether ITLN1's inhibitory effect on ovarian cancer cells' motility and invasive potential results from opposing the stimulating effect of LTF in culture media, we treated ovarian cancer cells with ITLN1 in culture media supplemented with 10% fetal bovine serum (FBS) in the presence of anti-LTF antibodies or IgG. In addition, we treated ovarian cancer cells with ITLN1 or PBS in serum-free media. ITLN1 did not inhibit ovarian cancer cell motility in either setting (Figures 5C and 5D). Finally, we treated SKOV3 and A224 ovarian cancer cells 100 μg/mL (a physiological level) of LTF in serum-free media. The results of a wound-healing assay showed a significant increase in cell motility, and the results of an invasion chamber assay showed a significant increase in invasion potential; however, when ITLN1 was added to the cultures, both the motility and the invasion rate were significantly decreased (Figures 5E and 5F). These data suggest that ITLN1 abrogates LTF's effect on ovarian cancer motility and invasive potential, and downregulation of ITLN1 allows LTF to enhance ovarian cancer cells' motility and invasive potential without opposition.

To examine the mechanism by which ITLN1 attenuates LTF's motility-promoting effect on ovarian cancer cells, we examined expression levels of key intermediate signaling molecules in the LTF/LRP1/MMP1 pathway in SKOV3 and A224. We discovered that LTF-treated SKOV3 and A224 showed marked increases in the levels of signaling molecules p-ERK1/2 (T202/Y204), total Jun, and p-Jun (S73) compared to cells treated with PBS in SFM (Fig. 6A). We also found marked decreases in expression levels of p-ERK1/2, total Jun and p-Jun in cells treated with LTF in the presence of ITLN1 compared with cells treated without ITLN1 (Fig. 6B). This showed that ITLN1 could abrogate LTF's effect on the activation of these signaling molecules. The roles of LRP1 and ERK activation in mediating the effect of LTF on MMP1 were further confirmed by silencing LRP1 (data no shown) and adding ERK inhibitor to SKOV3 and A224, respectively (Fig. 6C).

Specific Aim 2 Major Task 1. Because ITLN1 has been shown to increase insulin-dependent glucose uptake in adipocyte, we hypothesized that high levels of ITLN1 may suppress ovarian tumor growth by increasing glucose uptake by the visceral adipocytes in the omental microenvironment, thereby decreasing the glucose available to the neighboring ovarian cancer cells. We also hypothesized that the presence of ovarian cancer cells would lower both local and circulating ITLN1 levels, leading to decreased glucose uptake by the adipocytes, as well as increased local and circulating glucose levels that would fuel the ovarian cancer cells and support ovarian cancer progression. To test these hypotheses, we first confirmed that ITLN1 increased insulin-dependent glucose uptake only in mature

adipocytes (Figure 7A). We then sought to determine whether glucose played a role in mediating the growth-suppressive effect of ITLN1-treated adipocytes. The results showed that the growth-suppressive effect of ITLN1-treated mature adipocytes on SKOV3 and A224 cells was abrogated by the addition of glucose to the media (Figure 7B), which further confirmed the role of glucose in mediating ovarian cancer cell growth.

Next, we used qRT-PCR and Western blot analyses to evaluate the effect of ITLN1 on the expression of GLUT4/SLC2A4 – which is a key insulin–regulated facilitative glucose transporter – in mature adipocytes and to further delineate the mechanism by which ITLN1 increases glucose uptake in adipocytes. The results showed significantly higher levels of GLUT4 mRNA and protein expression in ITLN1-treated mature adipocytes than in controls (Figures 7C and 7D), suggesting that ITLN1 upregulates GLUT4 expression in adipocytes, leading to increased glucose uptake.

To test this hypothesis, we determined the amount of glucose uptake in mature adipocytes treated with ITLN1 in the presence of GLUT4-specific siRNAs (GLUT4 siRNA #1 and GLUT4 siRNA #2) or control scrambled siRNA. QRT-PCR and Western blot analyses confirmed successful knockdown of GLUT4 in mature adipocytes. The results also revealed a significantly smaller amount of glucose uptake in adipocytes transfected with GLUT4 siRNAs compared to those transfected with control siRNA (Figure 8A), suggesting that GLUT4 is essential for mediating the effect of ITLN1 on glucose uptake in adipocytes. Next, we sought to determine the role that GLUT4 expressed by adipocytes plays in ovarian cancer growth. Adipocytes transfected with GLUT4-specific siRNAs (GLUT4 siRNA #1 and GLUT4 siRNA #2) or with control scrambled siRNA were co-cultured with ovarian cancer cells in the presence of ITLN1. The results showed that the suppressor effect of ITLN1 on ovarian cancer cell growth was abrogated when GLUT4 was silenced in adipocytes (Figure 8B). These data suggest that ITLN1 suppresses ovarian cancer growth by increasing glucose uptake in adipocytes through the upregulation of GLUT4.

Specific Aim 2 Major Task 2. We originally proposed to use Induced Metabolic Bioluminescence Imaging to study the metabolic reprogramming of tumor microenvironment in the cyrosections of ovarian cancer tissue . We have identified a new approach based on Matrix-assisted Laser Desorption Ionization Mass Spectrometry Imaging (MALDI-IMS) which offers much higher spatial resolution than Induced Metabolic Bioluminescence Imaging. Uisng MALDI-IMS, we demosntrated that ITLN1 induced metabolic reprogramming in ovarian cancer cells by depriving glucose supply to cancer cells through increasing glucose uptake by the adipocyte in the omental tumor microenvironment in vivo (Figure 9).

Specific Aim 2 Major Task 3. Because we had demonstrated that omentin attenuating LTF mediated motility-inhibiting effect on ovarian cancer cells, we asked whether LTF also played a role in decreasing glucose uptake and GLUT4 expression in adipocytes. Our results demonstrated that mature adipocytes treated with LTF in serum-free media showed a significant decrease in GLUT4 mRNA expression levels and glucose uptake compared to those treated with PBS and the effects were completely abrogated by the addition of ITLN1 (Figures 8C and 8D). We also demonstrated that LTF promoted cell growth in ovarian cancer cells co-cultured with adipoytes in serum-free media and that the growth-promoting effect of LTF was abrogated when ITLN1 was added to the co-culture. These data suggest that decreased levels of ITLN1 allow LTF to downregulate GLUT4 and decrease glucose uptake in adipocytes without opposition, subsequently lead to enhanced tumor cell growth.

To determine whether ITLN1 plays a role in adipocyte-mediated metabolic reprogramming in ovarian cancer cells, which suppresses ovarian cancer cell growth, we performed a lactate secretion assay on SKOV3 and A224 cells co-cultured with either ITLN1-treated adipocytes or adipocytes alone. A significantly lower level of lactate secretion (a glycolysis product from Warburg effect) was observed in ovarian cancer cells co-cultured with ITLN1-treated adipocytes compared to those co-cultured with adipocytes alone (Figure 8E).

Specific Aim 3 Major Task 1. We employed a gene therapy approach to boost the circulating omentin levels in C57BL/6 mice using a custom-made adeno-associated virus (AAV-mITLN1), which transfers a constitutively expressed omentin gene to organs particularly the liver in the peritoneal cavity. We demonstrated that a single injection of our custom-made AAV-mITLN1 particles increased the serum level of ITLN1in C57BL/6 mice for up to 2 weeks (Figure 10). We did not pursue to use a adeno-associated vrus to boost circulating omentin level since we realized that the injection of recombinant omentin is a more promising approach after our initial pilot studies.

Specfic Aim 3 Major Task 2. To evaluate the effect of exogenous ITLN1 on ovarian cancer progression *in vivo*, we created orthotopic mouse models by injecting mouse ovarian cancer IG10 cells intraperitoneally into immunocompetent C57BL/6 mice. We first confirmed the effects of mouse recombinant ITLN1 protein on the migration rate of IG10 cells *in vitro.* Our results showed that mouse recombinant ITLN1 protein suppressed the migration rate of IG10 cells and downregulated MMP1 protein expression in IG10 cells. The effect was similar to that seen in human ovarian cancer cells. We then determined the optimal intraperitoneal injection concentration of mouse recombinant ITLN1 protein. First, one dose of mouse recombinant ITLN1 protein was injected intraperitoneally into IG10-bearing immunocompetent mice, and blood samples were collected from these mice at different time points. From 0 to 6 hours post-injection, the 100 μg/kg and 1 mg/kg injections did not cause a significant change in the circulating glucose concentration, but the 2 mg/kg injection resulted in a significant decrease (Figure 11A). Next, we used ELISA to further determine how long 2 mg/kg of mouse recombinant ITLN1 protein injected in ovarian cancer-bearing mice would be effective. The results showed that significant increases in circulating ITLN1 concentration were observed from 0 to 48 hours post-injection, and the mean ITLN1 concentration in ovarian cancer-bearing mice became comparable to the physiological ITLN1 concentration in mice without ovarian cancer 48 hours post-injection (means: 481.75 ng/mL and 495.87 ng/mL, respectively) (Figure 11B). The circulating glucose concentration in the cancer-bearing mice was also measured, and significant decreases were observed from 0 to 6 hours post-injection (Figure 11C). These data suggest that normal circulating ITLN1 levels can be achieved within 48 hours with one dose of recombinant ITLN1 protein (2mg/kg).

Next, we injected mouse recombinant ITLN1 protein (2 mg/kg) intraperitoneally into mouse ovarian cancer cell-bearing immunocompetent mice every 2 days for 6 weeks. The results showed a significant decrease in tumor growth rates in mice treated with ITLN1 (Figures 12A and 12B). The ascites volumes collected from mice treated with ITLN1 were also significantly lower than those for mice without ITLN1 treatment (Figure 12C). We found significantly higher circulating ITLN1 levels in the blood of ITLN1-treated mice compared to control mice (Figures 12D). ITLN1 treatment also reduced the expression of MMP1 insdie the tumor (Fig,12F).

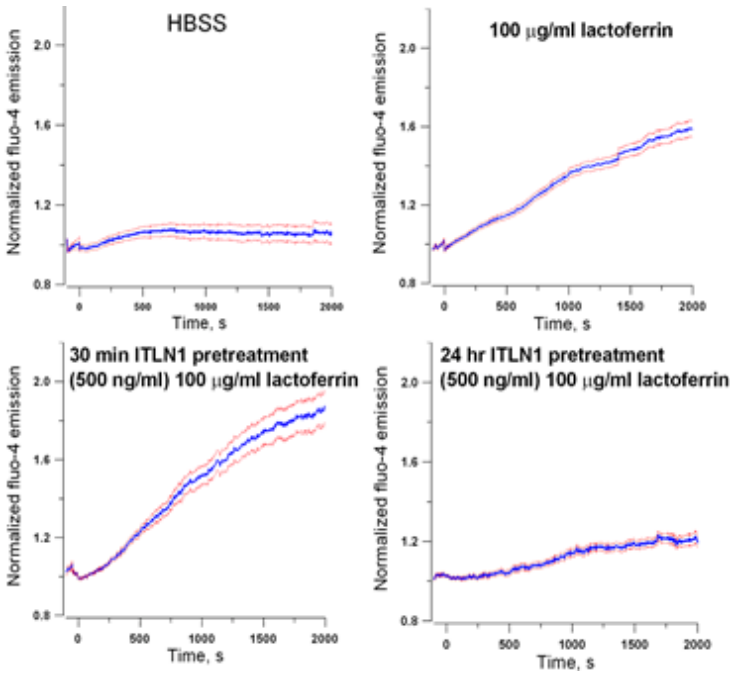

Figure 1. Graphs showing the mean normalized time course of cytosolic Ca^{2+} mobilization in A224 cells induced by lactoferrin. Cells were pretreated with omentin (ITLN1) or Hanks' Balanced Salt Solution (HBSS) for 30 min or 24 hours before lactoferrin was added to the bath of cells at t = 0 (mean ± SEM of four independent experiments for each treatment group).

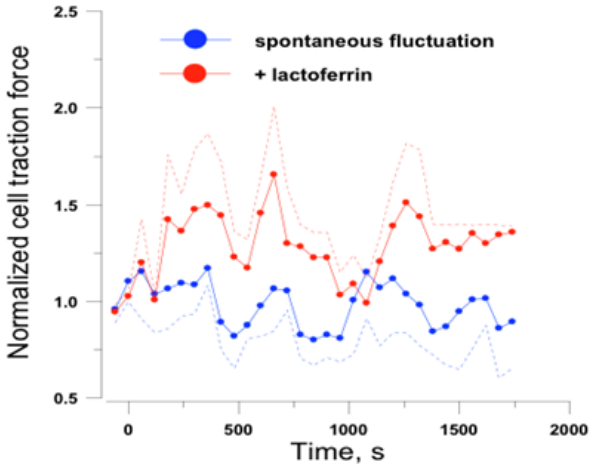

Figure 2. Mean normalized time course of cell traction force induced by lactoferrin (100 µg/ml) in A224 cells. Dotted lines are SEM (n = 6). Lactoferrin was applied to the cells at t = 0.

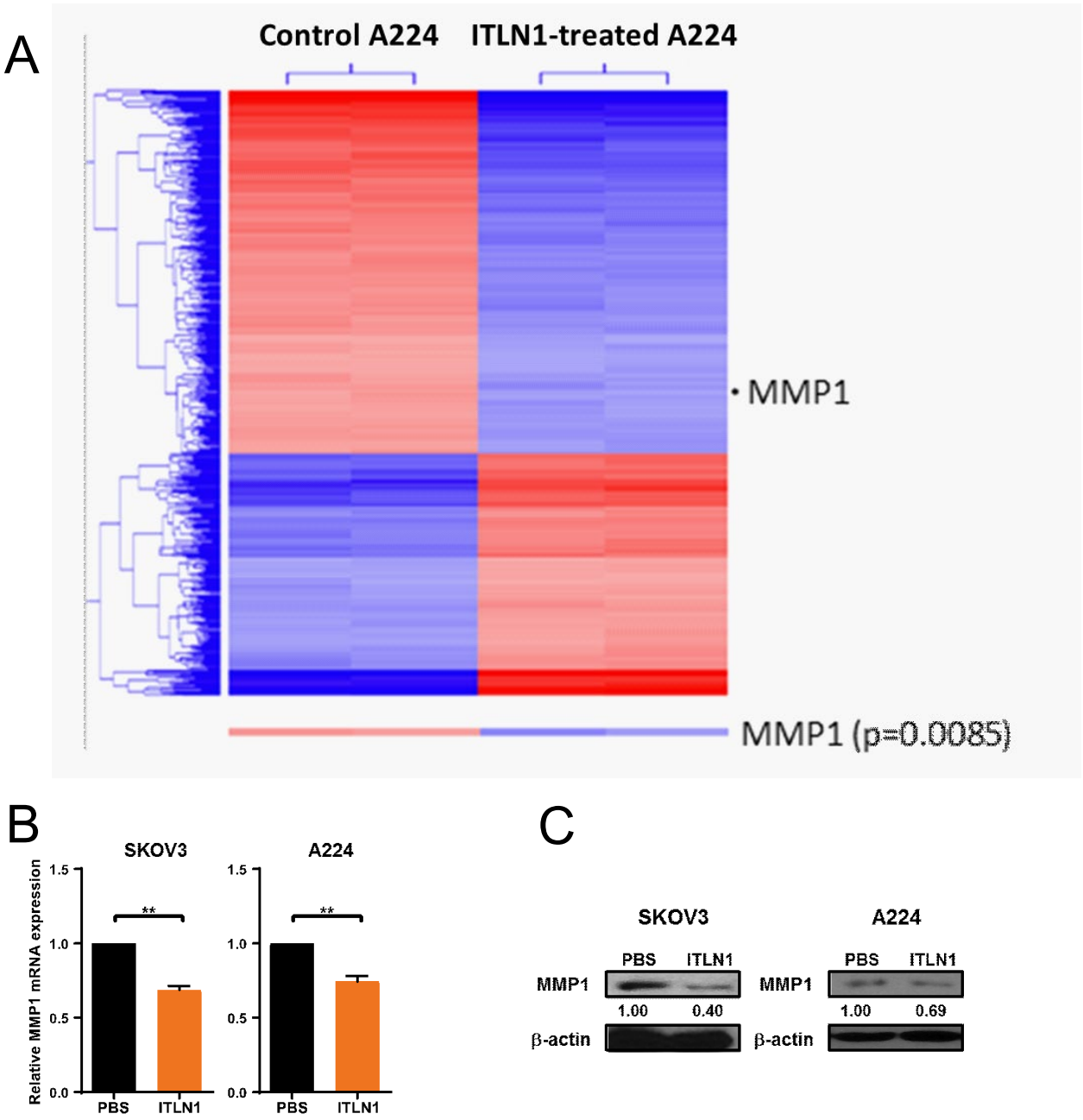

Figure 3. (A) Heat map from a transcriptome profiling analysis shows that MMP1 expression is significantly decreased in ITLN1-treated A224 cells (n=2) compared to control A224 cells without ITLN1 treatment (n=2). (B) Quantitative RT-PCR analysis shows a lower MMP1 mRNA level in ITLN1-treated SKOV3 and A224 cells compared to control cells treated with PBS. Results, as presented as mean±SD, show the average from at least three independent experiments. **p<0.01. (C) Western blot analysis shows a lower MMP1 protein level in ITLN1-treated SKOV3 and A224 cells compared to control cells treated with PBS. β-actin served as a loading control. Relative normalized protein levels with respect to the corresponding control are presented.

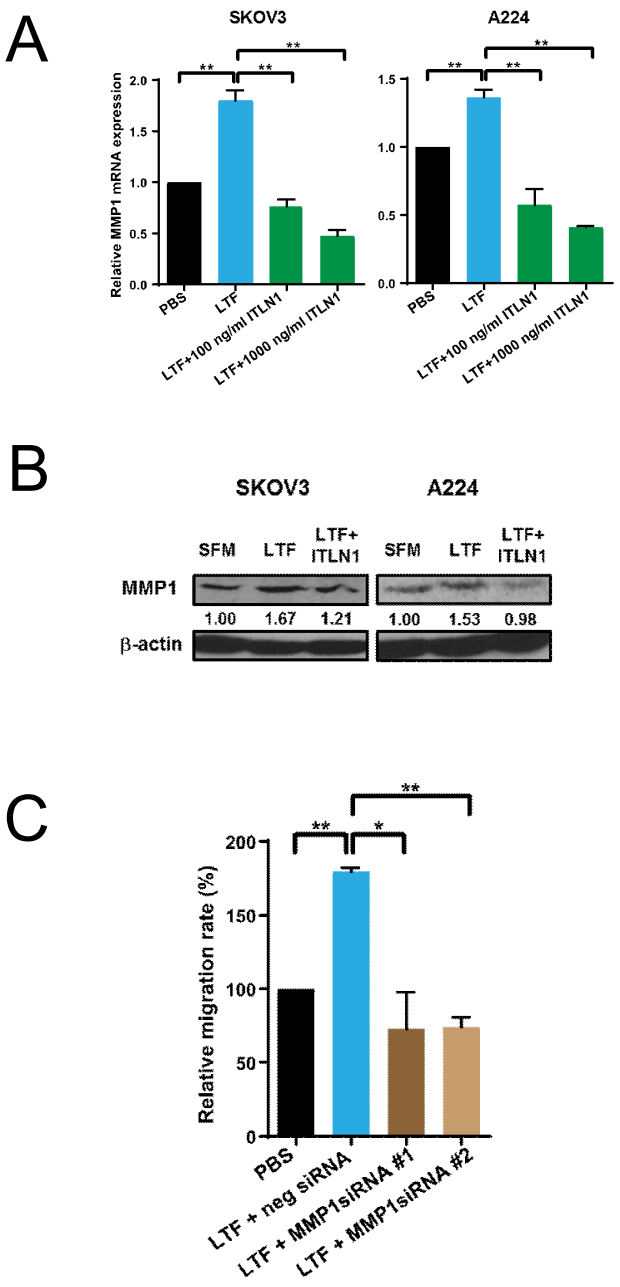

Figure 4. (A) Bar charts show that LTF upregulated the relative MMP1 mRNA expression in SKOV3 and A224 cells, while ITLN1 counteracted LTF's effect on MMP1 mRNA expression. Results, presented as mean±SD, show the average from at least three independent experiments. **p<0.01. (B) Western blot analysis shows that LTF upregulated MMP1 protein expression in SKOV3 and A224 cells, while ITLN1counteracted LTF's effect on MMP1 protein expression. β-actin served as a loading control. Relative normalized protein levels with respect to the corresponding control are presented. (C) LTF induces cell migration ability in SKOV3 and A224 cells compared to control cells, while MMP1 siRNAs counteracted the effect of LTF on cell migration. Results, presented as mean±SD, shows the average from at least three independent experiments with duplicated samples. *p<0.05; **p<0.01.

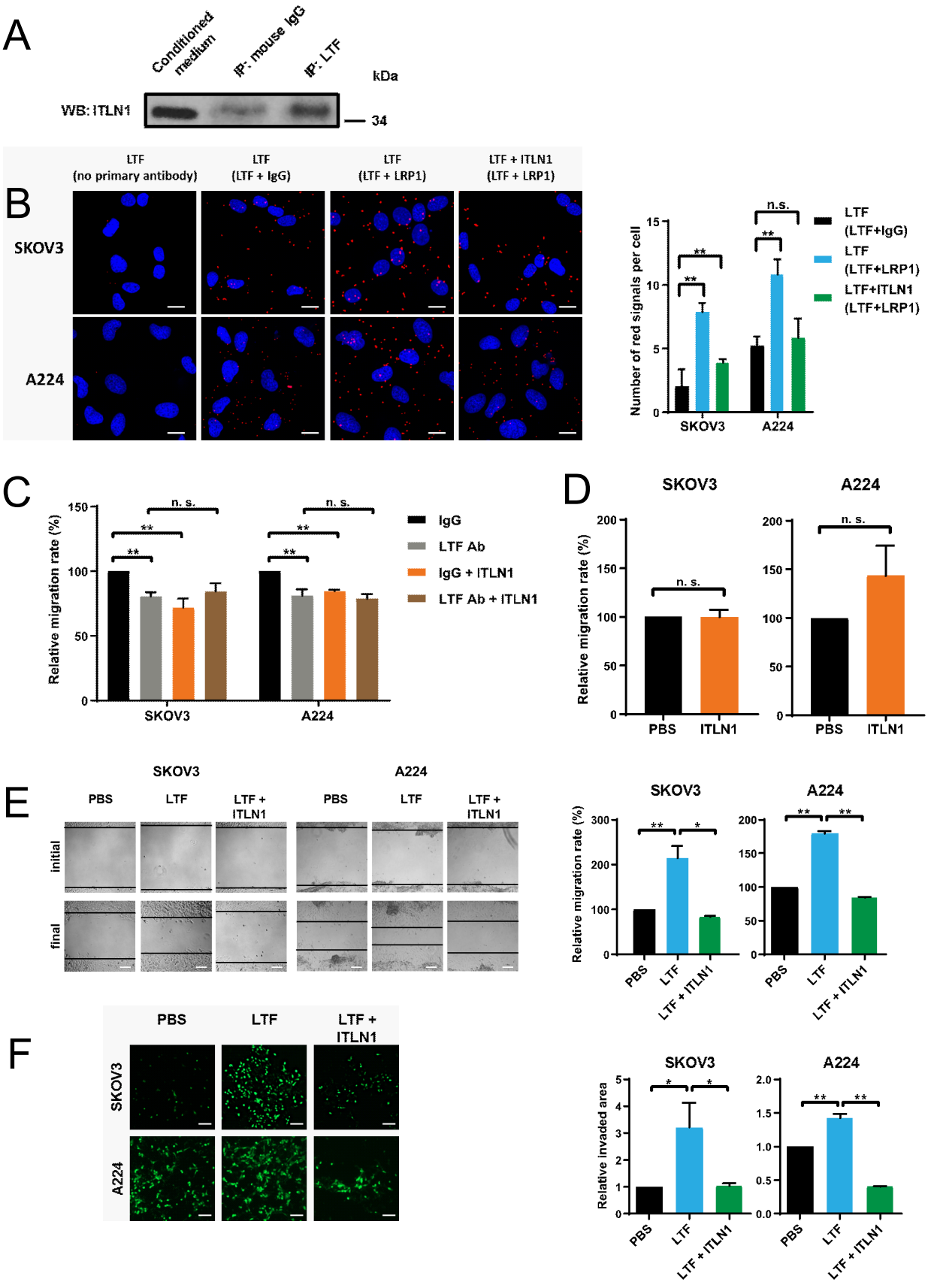
A
Conditioned medium
IP: mouse IgG
IP: LTF
kDa
WB: ITLN1
34
B
LTF (no primary antibody)
LTF (LTF + IgG)
LTF (LTF + LRP1)
LTF + ITLN1 (LTF + LRP1)
SKOV3
A224
Number of red signals per cell
LTF (LTF+IgG)
LTF (LTF+LRP1)
LTF+ITLN1 (LTF+LRP1)
n.s.
C
Relative migration rate (%)
IgG
LTF Ab
IgG + ITLN1
LTF Ab + ITLN1
n. s.
D
SKOV3
A224
Relative migration rate (%)
PBS
ITLN1
E
SKOV3
A224
PBS
LTF
LTF + ITLN1
initial
final
Relative migration rate (%)
F
Relative invaded area

Figure 5. (A) Western blot analysis shows ITLN1 on proteins pulled down by an anti-LTF antibody. Normal mouse IgG served as a control. ITLN1 band size=34 kDa.
(B) Representative microscopic images from a Duolink proximity ligation assay (PLA) on SKOV3 and A224 cells shows the interaction between LTF and LRP-1 while ITLN1 reduced the interaction. Red fluorescent signals indicate protein-protein interaction; nuclei were stained with 4,6-diamidino-2-phenylindole (DAPI) blue. Staining with no primary antibody and with anti-LTF antibody plus normal rabbit IgG served as controls. Bar=5 μm. Results in the bar chart, presented as mean±SD, show the average from at least three independent experiments. **p<0.01; n.s.=not significant (p>0.05).
(C) ITLN1 does not suppress cell migration ability in SKOV3 and A224 cells in LTF-depleted culture medium. Cells were treated with LTF antibody to deplete LTF in a culture medium with fetal bovine serum (FBS) before ITLN1 treatment. IgG was used as a control. Results are given as mean±SD. **p<0.01; n.s.=not significant (p>0.05).
(D) ITLN1 does not suppress cell migration ability in SKOV3 and A224 cells in FBS-free culture medium. Results are given as mean±SD. n.s.=not significant (p>0.05).
(E) Representative microscopic images show that LTF induced cell migration ability in SKOV3 and A224 cells compared to control cells, while ITLN1 counteracted LTF's effect on cell migration. Bar=50 μm. Results in the bar charts, presented as mean±SD, show the average from at least three independent experiments with duplicated samples. **p<0.01; *p<0.05.
(F) Representative microscopic images show that LTF induced cell invasion potential in SKOV3 and A224 cells compared to control cells, while ITLN1 counteracted the LTF's effect. Bar=50 μm. Results in the bar charts, presented as mean±SD, show the average from at least three independent experiments with duplicated samples. **p<0.01; *p<0.05.

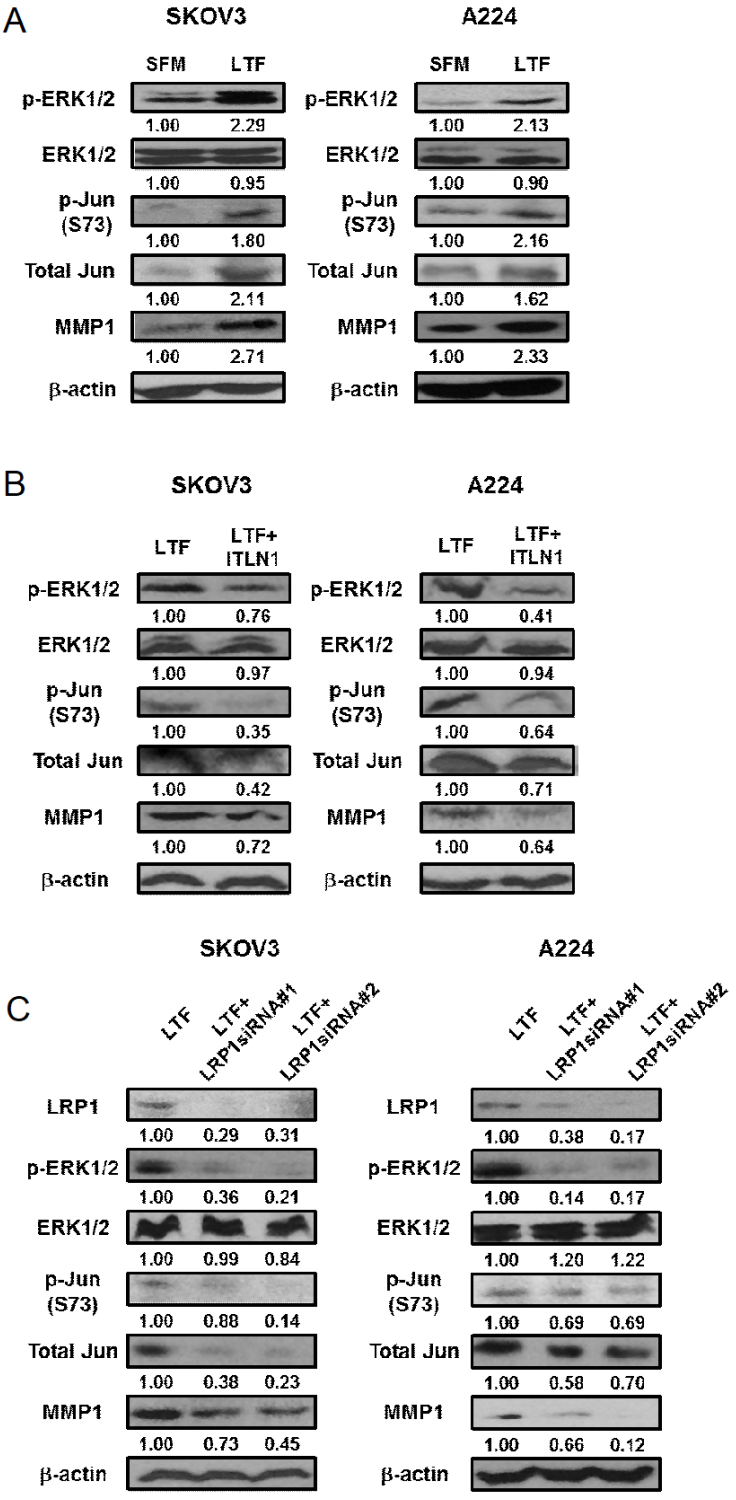

Figure 6. ITLN1 inhibits the LTF/LRP1/MMP1 signaling pathway. Western blot analyses show (**A**) higher protein levels of p-ERK1/2, p-Jun (S73), total Jun, and MMP1 in LTF-treated (100 μg/mL) SKOV3 and A224 compared to control cells without treatment; (**B**) lower protein levels of p-ERK1/2, p-Jun (S73), total Jun, and MMP1 in LTF-treated SKOV3 and A224 with ITLN1 (500 ng/mL) compared to control cells without ITLN1; and (**C**) lower protein levels of LRP1, p-ERK1/2, p-Jun (S73), total Jun, and MMP1 in LTF-treated SKOV3 and A224 with LRP1-specific siRNAs compared to control cells with negative siRNA. β-actin served as a loading control. Relative normalized protein levels with respect to the corresponding control are presented. Three independent experiments were performed.

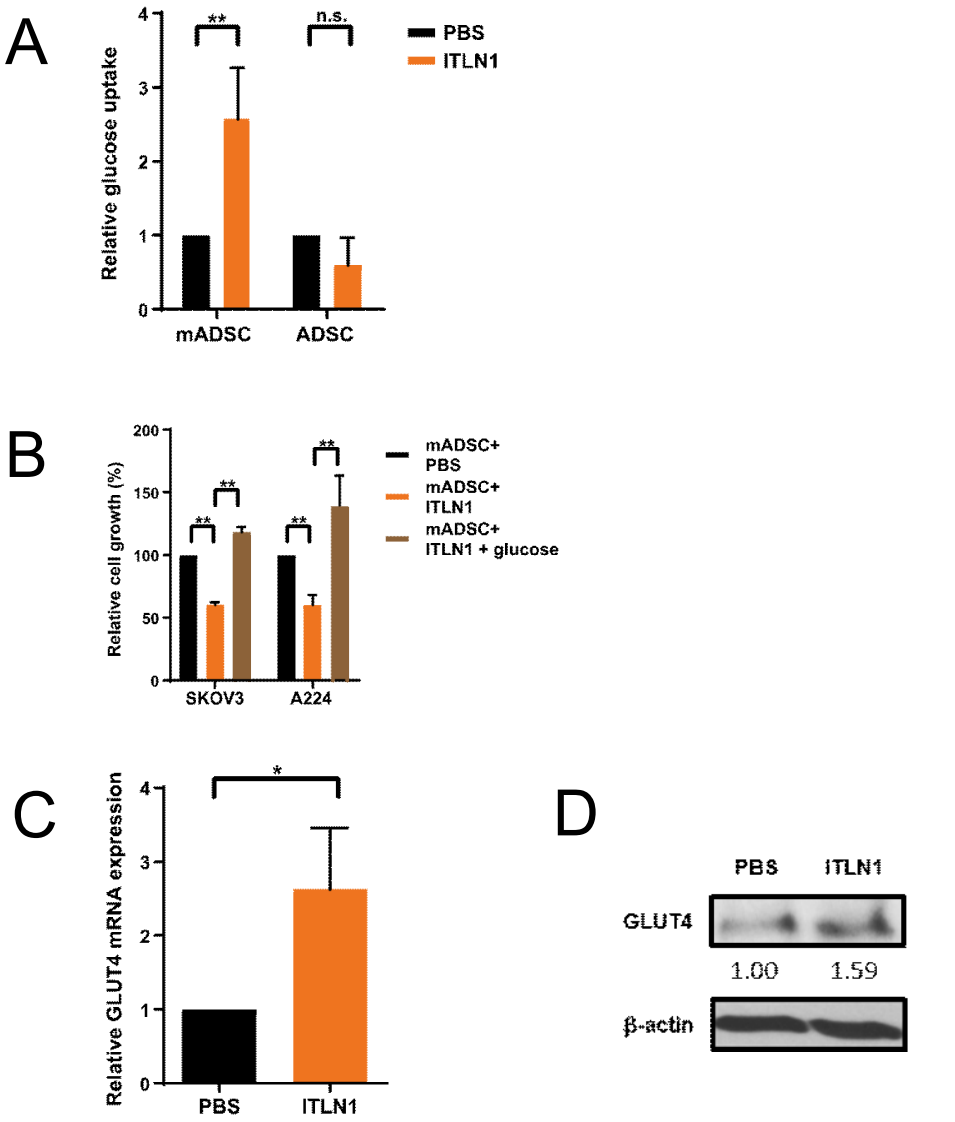

Figure 7. (A) ITLN1 enhanced insulin-dependent glucose uptake in mature adipocytes but not in adipose-derived stem cells (ADSC), when both are compared to control cells without ITLN1 treatment. Results, presented as mean±SD, show the average from three independent experiments. **p<0.01; n. s.=not significant (p>0.05). (B) Addition of glucose counteracts the effect of ITLN1 on cell growth in SKOV3 and A224 cells. Results, presented as mean±SD, show the average from three independent experiments. **p<0.01. (C) ITLN1 upregulated GLUT4 mRNA expression in mature adipocytes compared to control cells without ITLN1 treatment. Results, presented as mean±SD, show the average from three independent experiments. *p<0.05. (D) Western blot analysis shows a higher GLUT4 protein level in ITLN1-treated mature adipocytes compared to control cells. β-actin served as a loading control. Relative normalized protein levels with respect to the corresponding control are presented.

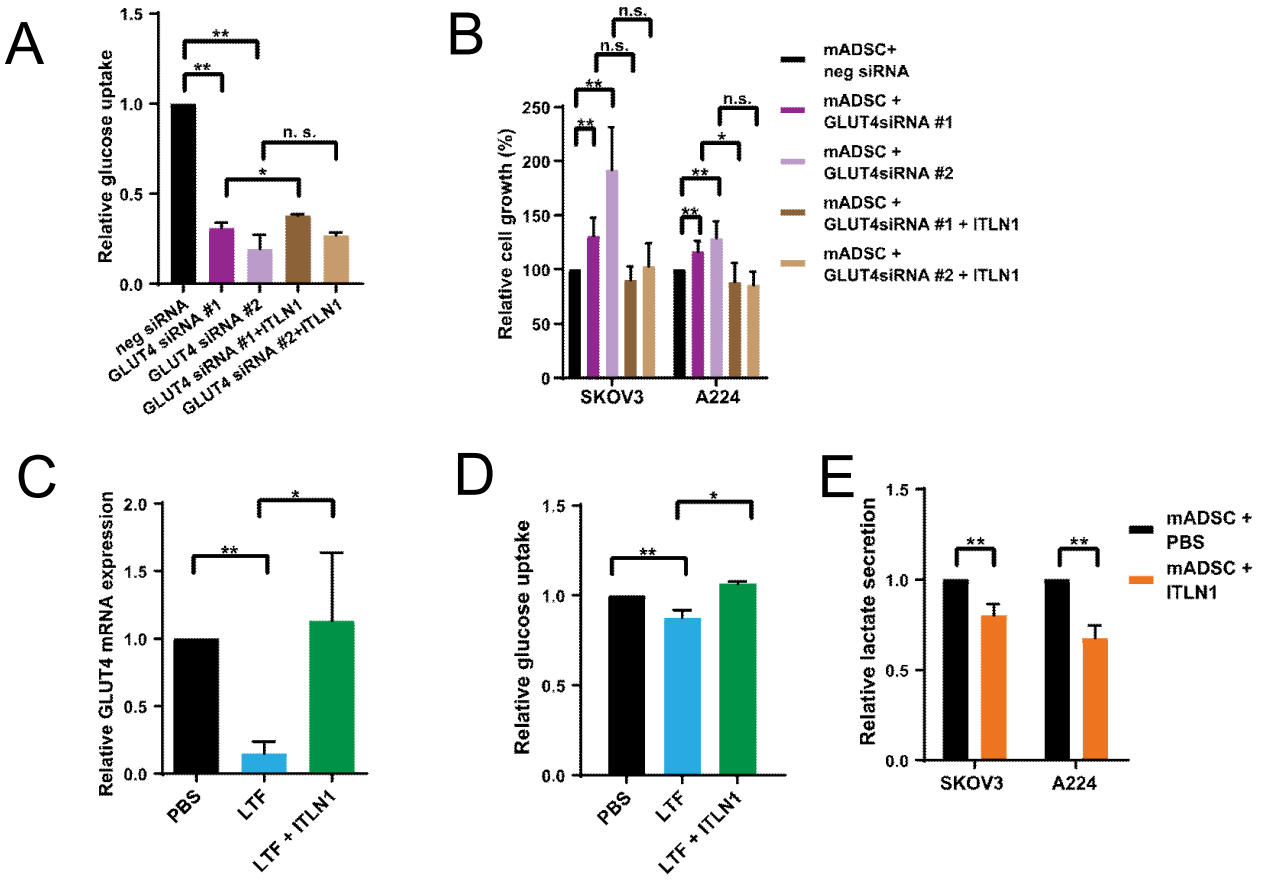

Figure 8. (A) GLUT4 siRNA transfection counteracted ITLN1's effect on insulin-dependent glucose uptake in mature adipocytes. Results, presented as mean±SD, show the average from at least three independent experiments. **p<0.01; *p<0.05; n. s.=not significant (p>0.05).
(B) GLUT4 siRNA transfection counteracted ITLN1's effect on cell growth in SKOV3 and A224 cells. Results, presented as mean±SD, show the average from at least three independent experiments. **p<0.01; *p<0.05; n. s.=not significant (p>0.05). (C) LTF downregulated the relative GLUT4 mRNA expression in mature adipocytes, while ITLN1 counteracted LTF's effect on GLUT4 mRNA expression. Results, presented as mean±SD, show the average from at least three independent experiments. p<0.01; *p<0.05. (D) LTF downregulated insulin-dependent glucose uptake in mature adipocytes, while ITLN1 counteracted the LTF's effect on glucose uptake. Results, presented as mean±SD, show the average from at least three independent experiments. **p<0.01; *p<0.05. (E) ITLN1 reduced lactate production in SKOV3 and A224 cells in the presence of mature adipocytes. Results, presented as mean±SD, show the average from at least three independent experiments. **p<0.01.

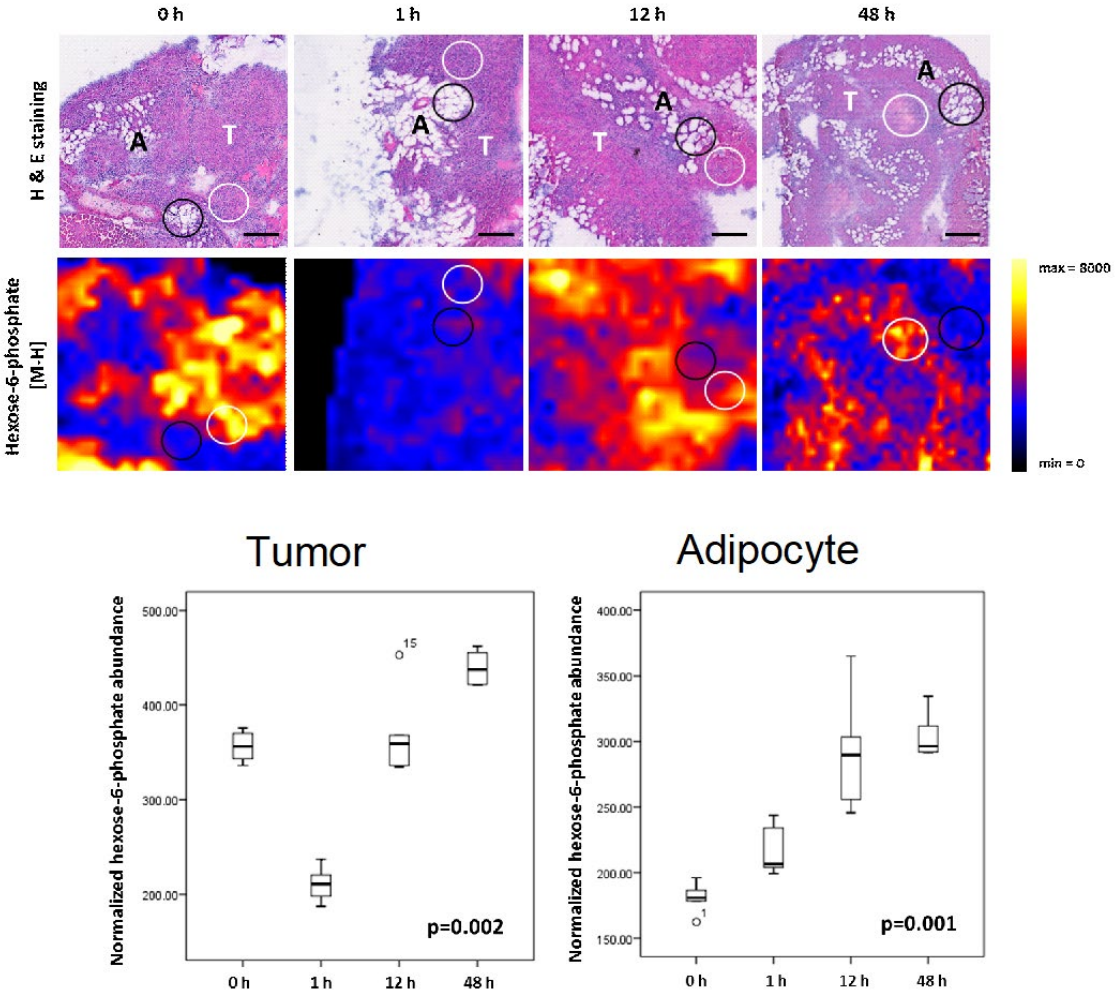

Figure 9. Representative images show reduced intensity of hexose-6-phosphate (glucose-6-phosphate and fructose-6-phosphate) (ion adduct: [M-H]; mass to charge ratio (m/z): 259.0224) in tumor cells (white circles) in frozen omental tumor tissue sections from 0 to 1 hours post-injection of ITLN1, while increased intensity of hexose-6-phosphate is seen in adjacent adipocytes (black circles) post-injection of ITLN1. The same tissue sections were stained with haematoxylin and eosin (H&E) after MALDI-imaging mass spectrometry (IMS). T=tumor cells; A=adipocytes; Bar=200 µm. Box plots show the normalized hexose-6-phosphate intensity in tumor cells and adipocytes at different time points after ITLN1 was intraperitoneally injected into C57BL/6 mice. n=5 in each group.

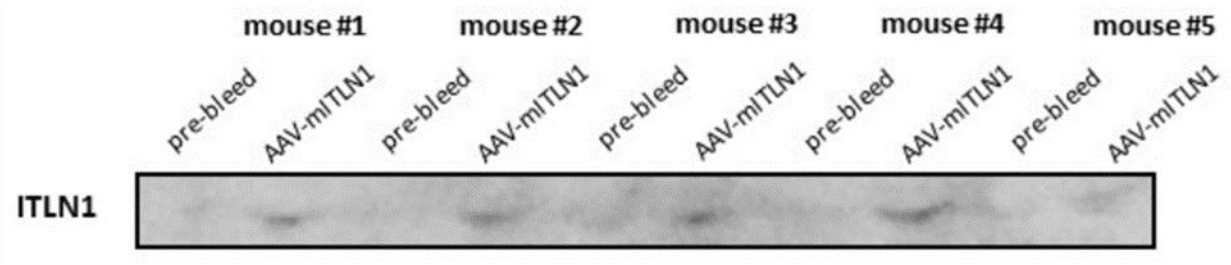

Figure 10. Western blots showing increase of serum omentin (ITLN1) level in mice two weeks after receiving a single injection of AAV-mLITN1 particles. Pre-bleed is the baseline.

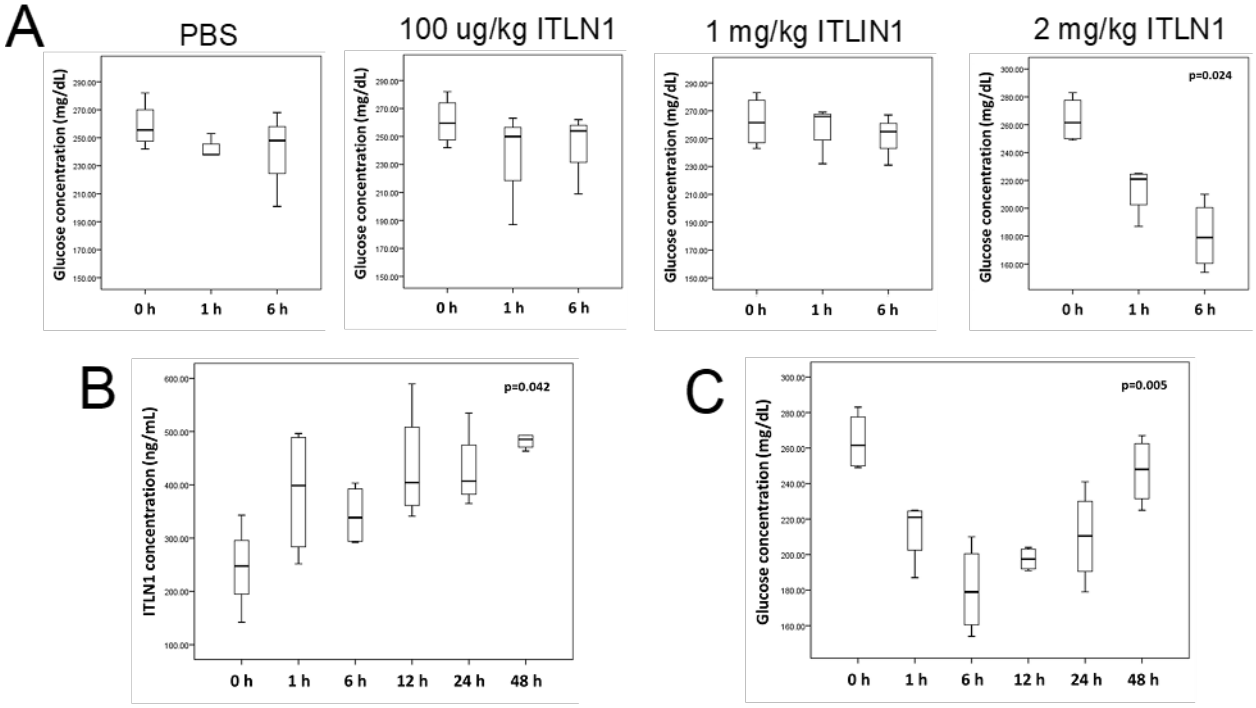

Figure 11. (A) Box plots shows a significantly lower glucose concentration in serum collected at different time points (0, 1 and 6 h) from IG10 cell-bearing C57BL/6 mice with PBS and ITLN1 injection (100 μg/kg, 1 mg/kg, and 2 mg/kg; n=5 in each group; p=0.024). (B) Box plot shows a significantly higher ITLN1 concentration in serum collected at different time points (0, 1, 6, 12, 24 and 48 h) from IG10 cell-bearing C57BL/6 mice with 2 mg/kg ITLN1 injection (n=5 in each group; p=0.042). (C) Box plot shows a significantly lower glucose concentration in serum collected at different time points (0, 1, 6, 12, 24 and 48 h) from IG10 cell-bearing C57BL/6 mice with 2 mg/kg ITLN1 injection (n=5 in each group; p=0.005).

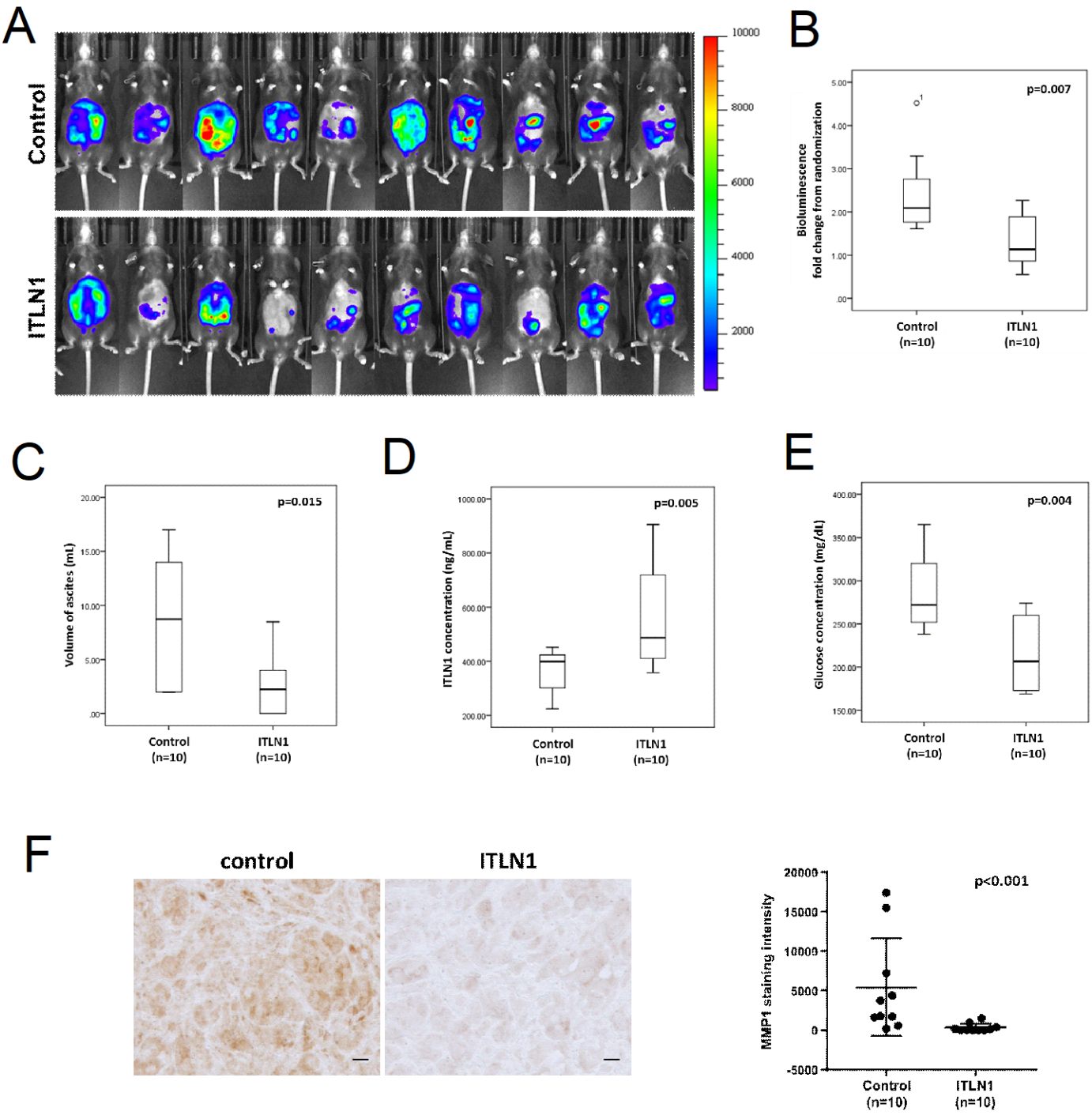

Figure 12. (A) Images show a decrease in bioluminescence of IG10 cell-bearing C57BL/6 mice with ITLN1 treatment (n=10) compared to untreated controls (n=10) six weeks after treatment. (B)-(E) Box plot shows a significantly (B) smaller tumor growth rate in; (C) smaller volume of ascites collected from; (D) higher ITLN1 concentration in serum collected from; and (E) lower glucose concentration in whole blood collected from IG10 cell-bearing C57BL/6 mice with ITLN1 treatment (n=10) compared to untreated controls (n=10) (p=0.007, p=0.015, p=0.005 and p=0.004, respectively) six weeks after treatment. (F) Representative microscopic images of paraffinized sections of tumor tissues collected from IG10 cell-bearing C57BL/6 mice six weeks after treatment shows a significantly lower MMP1 expression in the ITLN1 treatment group compared to the untreated controls. Bar=10 μm. Quantification of the staining intensity for each group (n=10) is shown in dot plot. p<0.001.

c. What opportunities for training and professional development has the project provided?

Nothing to report

d. How were the results disseminated to communities of interest?

Nothing to report. A manuscript was submitted to Nature Communication and is pending for acceptance.

e. What do you plan to do during the next reporting period to accomplish the goals?
A no cost extension has been approved due to the coronavirus outbreak. The project will end in 4/30/21. During the next reporting period (months 36-48), experiments proposed in Specific Aim 1 Major Task 1 using traction force microscope will be conducted and cell traction force map will be constructed as planned.

4. IMPACT

a. What was the impact on the development of the principal disciplines of the project?
Our study provides the insight into the functional role of omentin in the regulation of omental tumor microenvironment, and the development of obesity associated ovarian cancer. Our findings provide the proof-of-principle to develop novel therapeutic strategies based on induction or supplementation of omentin, including exercise and diet, in ovarian cancer patients, which will reduce ovarian cancer recurrent risk, suppress ovarian cancer progression, and thus improve patient survival rates.

b. What was the impact on other disciplines?
Nothing to report

c. What was the impact on technology transfer?
Nothing to report

d. What was the impact on society beyond science and technology?
Nothing to report

5. CHANGES/PROBLEMS

We originally proposed to use the Induced Metabolic Bioluminescence Imaging to study the metabolic reprogramming of tumor microenvironment in the cryosections of ovarian cancer tissue (Specific Aim 2 Major Task 2). We have identified an approach based on mass spectrometry (MALDI-IMS) which offers much higher spatial resolution. MALDI-IMS was thus used instead of Induced Metabolic Bioluminescence Imaging in Specific Aim 2 Major Task 2.

Protocol of MALDI-IMS: Sections from fresh-frozen mouse omental tumor tissues were obtained at 15 μm thickness in a cryostat and mounted on glass microscope slides. HTX Sprayer M5 (HTX Technologies, LLC., Chapel Hill, NC, USA), an automated sprayer matrix applicator was used to coat the tissue sections with 10 mg/mL 1,5-diaminonaphthalene (Sigma-Aldrich) as the MALDI matrix dissolved in 90/10 acetonitrile/water. The slides were scanned using an EPSON scanner (Epson, Suwa, Japan), and the areas of interest were mapped into High Definition Imaging software (Waters, Milford, MA, USA) before being loaded into the mass spectrometer. Imaging of tissue sections was achieved with a SYNAPT G2-Si high resolution mass spectrometer with a MALDI source interface (Waters), specifically configured for imaging biological and chemical materials. The scanner used a 2.5 kHz Nd:YAG solid state laser that rastered across the tissue sample, giving a chemical composition profile for each corresponding spatial coordinate. These mass spectral data were collated by the software to produce a chemical image that could be correlated with the sample histological profile. The laser power was set to 250 (arbitrary units) with 300 laser shots per pixel of data. The laser raster step was set to 60 μm to match the laser spot size

of 60 μm. The instrument was checked for mass accuracy using red phosphorus and calibrated with the m/z range from 50 to 1000 before acquiring the data. After negative mode acquisition, the software automatically processed the raw data into a collection of images. Metabolite identifications were made based on accurate mass, which typically has a discrepancy of less than 1 ppm. Masses were searched against the Human Metabolome Database for identifications.

6. PRODUCTS

Conference Abstracts: presented in 2019 Experimental Biology

a. Yip, Kay-Pong , Chi Lam Au-Yeung, Samuel C. Mok. Interactions of Omentin and Lactotransferrin in the Progression of Metastatic Ovarian Cancer. FASEB J, 2019.
b. Yip, Kay-Pong, Byeong Cha, Omkar Paudel, Samuel C. Mok, and James S.K. Sham. Mobilization of Intracellular Calcium Stores and ER-Mitochondrial Coupling in High-grade Serous Ovarian Cancer (HGSOC) Cells. FASEB J, 2019.

7. PARTICIPANTS & OTHER COLLABORATING ORGANIZATIONS

a. What individuals have worked on the project?

Kay-Pong Yip: no change
Samuel C. Mok: no change

b. Has there been a change in the active other support of the PD/PI(s) or senior/key personnel since the last reporting period?

Nothing to report

c. What other organizations were involved as partners?

Organization Name: N/A
Location of Organization: N/A
Partner's contribution to the project: N/A
Financial support: N/A
In-kind support: N/A
Facilities: N/A
Collaboration: N/A
Personnel exchanges: N/A
Other:

8. SPECIAL REPORTING REQUIREMENTS

No applicable

9. APPENDICES

a. Yip, Kay-Pong , Chi Lam Au-Yeung, Samuel C. Mok. Interactions of Omentin and Lactotransferrin in the Progression of Metastatic Ovarian Cancer. FASEB J, 2019.
b. Kay-Pong Yip, Byeong Cha, Omkar Paudel, Samuel C. Mok, and James S.K. Sham. Mobilization of Intracellular Calcium Stores and ER-Mitochondrial Coupling in High-grade Serous Ovarian Cancer (HGSOC) Cells. FASEB J, 2019.

4622

Interactions of Omentin and Lactotransferrin in the Progression of Metastatic Ovarian Cancer

Kay-Pong Yip[1], Chi Lam Au-Yeung[2], Samuel C Mok[2]

[1]University of South Florida, Tampa, FL, [2]The University of Texas MD Anderson Cancer Center, Houston, TX

Advanced stage serous ovarian cancer metastasizes preferentially to the omentum, which is a major site of intra-abdominal fat accumulation and is covered by a layer of mesothelial cells (mesothelium). Ovarian cancer cells first adhere to and then penetrate through the mesothelium. It was previously shown the expression of adipokine omentin (ITLN1) in mesothelial cells was down-regulated when mesothelial cells were co-cultured with ovarian cancer cells. Survival correlation studies demonstrated that patients with serum ITLN1 levels of >350 ng/mL at the time of first treatment experienced longer survival times than those with lower levels of ITLN1. In addition, wound-healing assay and invasion assay demonstrated that ovarian cancer cells (SKOV3 and A224) treated with physiological levels of ITLN1 showed a significant decrease in motility and invasion potential. However, the molecular mechanism by which ITLN1 modulates these malignant phenotypes remains unknown. Cancer cells migrate using cell-matrix mechanocoupling mechanisms through paths generated by the degradation and remodeling of the extracellular matrix (ECM) and by force-mediated deformation (powered by cell traction force from cancer cells). To explore whether omentin suppresses ovarian cancer invasion potential via inhibiting ECM proteolysis, RNA sequencing and pathway analyses were performed on ITLN1 treated cancer cells. Significantly lower levels of MMP1 (matrix metalloproteinase-1) was found in cancer cells treated with ITLN1 than untreated cells, which was confirmed by qRT-PCR analysis. Since ITLN1 has been shown to interact with LTF (lactotransferrin), and binding of LTF to its receptors LRP1 (low-intensity lipoprotein-receptor-related protein 1) can transcriptionally upregulate MMP1, an i*n vitro* pull-down assay on purified LTF and recombinant ITLN1 in serum-free media was first performed to confirm that ITLN1 interacts and binds with LTF. To determine whether ITLN1 can interfere with the binding of LTF to LRP1 on ovarian cancer cells, a Duolink proximity ligation assay was performed using both anti-LTF and anti-LRP1 antibodies. There was a significant decrease in fluorescent signals in cells that were treated with ITLN1 compared to the control. The results suggested that ITLN1 interacts with LTF and prevents LTF from binding to its receptor LRP1 on ovarian cancer cells. Furthermore, ITLN1 abrogated the effects of LTF on MMP1 expression in a dose-dependent manner in ovarian cancer cells. LTF not only induced MMP1 expression, but also triggered an increase of cytosolic Ca^{2+} and cell traction force in ovarian cancer cells, which were attenuated by pre-incubation with ITLN1. Taken together, these data suggest that ITLN1 suppressed LTF's effect on the motility and invasion potential of ovarian cancer cells by decreasing MMP1 expression and cell traction force generation through modulating a calcium dependent LTF-LRP1 signaling pathway.

Support or Funding Information

Department of Defense : grant W81XWH-17-1-0146

Print Close

4929

Mobilization of Intracellular Calcium Stores and ER-Mitochondrial Coupling in High-grade Serous Ovarian Cancer (HGSOC) Cells

Kay-Pong Yip[1], Byeong Cha[1], Omkar Paudel[2], Samuel C. Mok[3], James S.K. Sham[2]

[1]Department of Molecular Pharmacology and Physiology, University of South Florida, Tampa, FL, [2]Johns Hopkins University School of Medicine, Baltimore, MD, [3]Department of Gynecologic Oncology and Reproductive Medicine, University of Texas MD Anderson Cancer Center, Houston, TX

Ca^{2+} signaling plays crucial roles in cancer metastasis by participating in proliferation, migration, invasion and transformation. However, specific involvements of various intracellular Ca^{2+} stores in these processes are not clearly defined, and the characteristics of the Ca^{2+} release mechanisms have not been determined in high-grade ovarian cancer (HGSOC) cells. In the present study, we sought to determine the functional properties of the IP_3-receptor (IP_3R), ryanodine receptor (RyR), and nicotinic acid adenine dinucleotide phosphate (NAADP) gated Ca^{2+} release pathways in the HGSOC cell line OVCA433. Subcellular Ca^{2+} signals in OVCA433 cells were monitored using confocal fluorescence microscopy with the cytoplasmic Ca^{2+} fluorescent dye Fluo-4 AM. Activation of IP_3R by photorelease of cell-permeant caged-IP_3 using a 405 laser elicited a dramatic increase in cytosolic [Ca^{2+}] indicating robust IP_3R-gated Ca^{2+} stores. Activation of RyRs using the common agonist caffeine or 4-chloro-m-cresol (4CmC) activated rapid Ca^{2+} release, indicating the presence of functional RyR-gated Ca^{2+} stores in these non-excitable cells. Moreover, application of the cell permeant NAADP-AM also caused intracellular Ca^{2+} release. These results demonstrated the presence of functional IP_3R-, RyR-, and NAADP-gated Ca^{2+} stores in OVCA433 cells. Super-resolution confocal live cell imaging were preformed in OVCA433 cells loaded with Bodipy-FI-X ryanodine, CellLight ER-RFP, Lysotracker Deep Red, and/or Mitotracker Orange, to further examined the subcellullar organization of the intracellular Ca^{2+} stores. We found that RyRs are expressed in a subpopulation of ER occupying special locations in the central and peripheral regions, and the ERs in the central region are closely associated with mitochondria. The lysosomal acidic stores are distributed in a random manner. The close association of central ERs and mitochondria suggests that ER-mitochondrial coupling may occur in OVCA433 cells. This possibility was confirmed by photorelease of caged-IP_3 in a small region inside the cells by an UV laser which elicited significant increase in $[Ca^{2+}]_{mito}$ measured by Rhod-2. Application of caffeine to OVCA433 cells also elicited a rapid increase in cytosolic [Ca^{2+}], which was followed by sustained increase in $[Ca^{2+}]_{mito}$. Moreover, caffeine-induced Ca^{2+} release activated superoxide bursts in mitochondria of OVCA433 cells loaded with the mitochondrial ROS indicator dye MitoSOX Red. Our results, hence, for the first time, characterized the IP_3R-, RyR-, and NAADP-mediated Ca^{2+} release, and demonstrated IP_3R and RyR-dependent ER-mitochondrial Ca^{2+} transfer and coupling in OVCA433 cells. The results provide the fundamental information on intracellular Ca^{2+} signaling in HGSOC cells and could be important for the study of Ca^{2+} signaling in ovarian cancer metastasis.

Support or Funding Information

Supported by DOD W81XWH-17-1-0146